Operator ordering in effective-mass theory for heterostructures. I. Comparison with exact results for superlattices, quantum wells, and localized potentials

G. T. Einevoll, P. C. Hemmer, and J. Thomsen
Institutt for Fysikk, Norges Tekniske Høgskole, Universitetet i Trondheim, N-7034 Trondheim, Norway
(Received 9 February 1990)

We study, for heterostructures with abrupt interfaces, the problem of operator ordering in the effective-mass Hamiltonian with kinetic-energy operator $\frac{1}{2}m^{\alpha}\mathbf{p}m^{\beta}\mathbf{p}m^{\alpha}$, for a position-dependent effective mass. Here, $2\alpha+\beta=-1$. Through exact model calculations on superlattices, quantum wells, and localized potentials we show that when effective-mass theory is applicable, $\alpha=0$ and $\beta=-1$. In all cases the effective-mass theory has the status of an asymptotically exact treatment, except for strained lattices.

I. INTRODUCTION

A simple and extensively used method for determining electronic states and other properties in semiconductor physics is the effective-mass approximation, by means of which the complexities due to the periodic potential are hidden in the effective-mass tensor. The effective-mass theory was originally developed[1] to treat impurities in an otherwise perfect crystal, and the treatment has been shown to be asymptotically exact when the variations of the perturbations of an otherwise perfect crystal are sufficiently small over a unit cell.

In its simplest form the one-electron wave function (envelope function) for impurity state close to the conduction band obeys the Schrödinger equation with a Hamiltonian

$$H=-\frac{\hbar^2}{2m}\nabla^2+E^c+U(\mathbf{r}) . \tag{1}$$

Here, m is the effective mass (considered a scalar here), E^c is the single minimum of the energy dispersion function $E(\mathbf{k})$, and $U(\mathbf{r})$ is the perturbation of the periodic crystal.

As a result of the recent development of crystal-growth techniques for the production of nonuniform semiconductor specimens, the effective-mass method has also been used extensively as a computational tool for such heterostructures.[2] It is possible to produce, by means of the molecular-beam-epitaxy technique, for example, abrupt interfaces between materials, and for such layered systems the conduction-band edge E^c and the effective mass m become position dependent. The most straightforward generalization of Eq. (1) uses the position-dependent band edge $E^c(\mathbf{r})$ in the potential-energy part of the Hamiltonian. Since, however, a position-dependent effective mass $m(\mathbf{r})$ and the momentum operator $\mathbf{p}$ do not commute, a question concerning the correct form for the kinetic-energy operator arises.[3-17]

The basic requirement is, of course, that the Hamiltonian is Hermitian. The class of operators

$$H_{\rm kin}=\tfrac{1}{4}\sum_i c_i(m^{\alpha_i}\mathbf{p}m^{\beta_i}\mathbf{p}m^{\gamma_i}+m^{\gamma_i}\mathbf{p}m^{\beta_i}\mathbf{p}m^{\alpha_i}) , \tag{2}$$

where $\alpha_i+\beta_i+\gamma_i=-1$ and where the coefficients c_i sum to unity, are all Hermitian quantum-mechanical operators corresponding to the classical kinetic-energy expression $p^2/2m$.

Equation (2) includes special cases that have appeared in the literature,[3] viz.,

$$\tfrac{1}{4}m^{-1}p^2+\tfrac{1}{4}p^2m^{-1};\ \tfrac{1}{2}m^{-1/2}p^2m^{-1/2};\ \tfrac{1}{2}\mathbf{p}m^{-1}\mathbf{p} . \tag{3}$$

In order to apply the effective-mass method, one has to know the values of the parameters occurring in (2). One can contemplate several ways of accomplishing this.

As a first question, one can ask whether there are any *inherent* limitations on the kinetic operators (2). In a recent article,[11] we investigated the Schrödinger equation with (2) as the kinetic operator, and showed that the many-term operator (2) is equivalent to a two-term operator[12]

$$H_{\rm kin}=\tfrac{1}{4}m^{\alpha}\mathbf{p}m^{\beta}\mathbf{p}m^{\gamma}+\tfrac{1}{4}m^{\gamma}\mathbf{p}m^{\beta}\mathbf{p}m^{\alpha} , \tag{4}$$

and, in a model calculation, we demonstrated that $\alpha\neq\gamma$ gives *divergent* energy eigenvalues for heterostructures with abrupt interfaces, on physical grounds an unacceptable result. One is thus led to consider the restricted form

$$H=\tfrac{1}{2}m^{\alpha}\mathbf{p}m^{\beta}\mathbf{p}m^{\alpha}+E_c(\mathbf{r})+U(\mathbf{r}) \tag{5}$$

as a possible candidate for an effective-mass Hamiltonian for heterostructures. It is a one-parameter family of operators, since $2\alpha+\beta=-1$.

According to Morrow's analysis,[4] the works of White and Sham[13] and of Kahen and Leburton[14] correspond to the case with $\alpha=0$ and $\beta=-1$, while the works of Zhu and Kroemer[15] and of Ando and Mori[16] correspond to the case with $\alpha=-\frac{1}{2}$ and $\beta=0$.

In Ref. 11 we also presented a consistency argument in favor of the values $\alpha=\gamma=0$, or, equivalently, $\beta=-1$. The argument was based upon an application of Eq. (5) to a test case, a δ-function potential $U(\mathbf{r})$ situated at the interface between two materials. The δ function was considered as the limit of narrow and deep square wells, and the bound-state energy turned out to be independent of

the actual limiting procedure if and only if $\beta=-1$. This type of argument remains in the class of criteria inherent to the effective-mass Hamiltonian. Since it is based on a rather special situation involving a singular potential, it may not be completely convincing. We therefore keep an open mind, and accept at this stage all possible parameter values for β in Eq. (5).

A second approach for determining the value of β is to compare, for a solvable test case, exact results with effective-mass results, parametrized by β. This is the strategy of the present article. The strategy is based upon a belief that the value of β is universal. If β were not universal, the usefulness of an effective-mass equation would be severely limited. We will test to some extent the universality of the results by varying the parameters of the model, and also by considering different physical situations. In Sec. II we treat model superlattices, in Sec. III we specialize to a single quantum well, and in Sec. IV we consider a local impurity potential in a heterostructure. A short note on the impurity potential case has already appeared.[17]

We select as test models binary heterostructures with an abrupt interface, since this is the case usually encountered in practice. For analytic convenience, the homogeneous materials are one-dimensional Kronig-Penney lattices.

It is a distinct possibility that for *no* values of the parameters will the Hamiltonian (5) yield results in agreement with the exact solutions. If so, we must conclude that effective-mass theory—at least in the form considered here—is not a valid description. As will be demonstrated below, the effective-mass treatment does not always have the status of an asymptotically exact theory, but we show that *when* it is applicable, the Hamiltonian (5) with

$$\alpha=0, \quad \beta=-1 \tag{6}$$

should be used.

The prescription (6) has been used previously, often with no justification beyond hermiticity. Derivations in the literature have been based upon assumptions too restrictive for applications to heterostructures with abrupt interfaces. Sometimes current conservation is used as an argument for some definite operator ordering. We want to point out that a conclusive argument for heterostructures with abrupt interfaces cannot be cased on current conservation. It is straightforward to show that the probability current corresponding to the Hamiltonian (5) is

$$\mathbf{j}=\hbar m^{\alpha+\beta}\mathrm{Im}(\phi^*\nabla m^{\alpha}\phi) \ .$$

At an *abrupt* interface between two homogeneous materials 1 and 2, the requirement of current conservation reduces to

$$\frac{1}{m_1}\phi_1^*\nabla\phi_1=\frac{1}{m_2}\phi_2^*\nabla\phi_2 \ ,$$

independent of α,β. Hence arguments based upon current conservation *cannot* settle the operator-ordering question.

II. SUPERLATTICES

A. Exact solution of the microscopic problem

Our test model of a superlattice is a binary heterostructure consisting of alternating regions of materials 1 and material 2 (Fig. 1). The widths of the material 1 (2) regions are p_1a_1 (p_2a_2), where a_1 (a_2) is the lattice constant in material 1 (2), and the p_i's are integers.

For analytic convenience each of the homogeneous regions is a one-dimensional Kronig-Penney lattice, with a δ-function well placed in the center of the unit cells of the separate materials. The potential level in between the wells is denoted by V_1 (V_2) in material 1 (material 2). The periodic potential $V(x)$ is sketched in Fig. 2.

We parametrize the potential by dimensionless strength parameters α_i as follows:

$$V(x)=\begin{cases} V_1-\dfrac{\hbar^2\alpha_1}{m_0a_1}\displaystyle\sum_{n=1}^{p_1}\delta(x-(n-\tfrac{1}{2})a_1) \\ \qquad\qquad \text{for } 0\le x<p_1a_1 \\ V_2-\dfrac{\hbar^2\alpha_2}{m_0a_2}\displaystyle\sum_{n=1}^{p_2}\delta(x-(n-\tfrac{1}{2})a_2-p_1a_1) \\ \qquad\qquad \text{for } p_1a_1\le x\le p_1a_1+p_2a_2 \end{cases} \tag{7}$$

in the first superlattice unit cell $(0,p_1a_1+p_2a_2)$. The origin is chosen arbitrarily at the left-hand side of a material-1 layer. Here, m_0 denotes the free-electron mass.

The exact solution for the microscopic Schrödinger equation proceeds by standard transfer-matrix techniques. We introduce dimensionless transfer matrices $\underline{T}_i$ which connect the wave function ψ and its derivative $a_i\psi'$ at a position a distance $\frac{1}{2}a_i$ on the left-hand side of a δ-function well in material i with the same quantities at a position $\frac{1}{2}a_i$ on the right-hand side of the same δ-function well. For example,

$$\begin{pmatrix} \psi(a_1) \\ a_1\psi'(a_1) \end{pmatrix}=\underline{T}_1\begin{pmatrix} \psi(0) \\ a_1\psi'(0) \end{pmatrix} . \tag{8}$$

For Kronig-Penney materials these transfer matrices have a simple form:

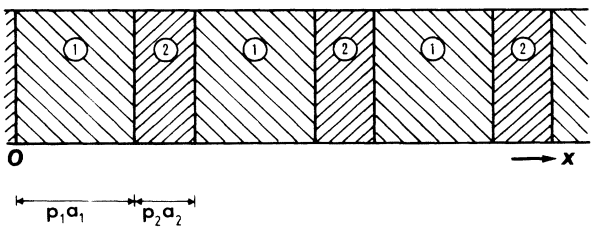

FIG. 1. The binary superlattice.

$$\underline{T}_i(q_i)=\begin{bmatrix} \cos q_i-\alpha_i q_i^{-1}\sin q_i & q_i^{-1}\sin q_i-\alpha_i q_i^{-2}+\alpha_i q_i^{-2}\cos q_i \\ -q_i\sin q_i-\alpha_i-\alpha_i\cos q_i & \cos q_i-\alpha_i q_i^{-1}\sin q_i \end{bmatrix} . \tag{9}$$

Here the dimensionless quantity q_i is determined by the energy eigenvalue E through

$$\frac{\hbar^2}{2m_0 a_i^2}q_i^2=E-V_i , \tag{10}$$

and may be real or imaginary. We have used $a_i\psi'$ as the lower component of the state vector in order to have completely dimensionless transfer matrices. There is a price to pay for this. At the boundary between material 1 and material 2 we must transform from one type of state vector to another:

$$\begin{bmatrix} \psi \\ a_i\psi' \end{bmatrix}=\begin{bmatrix} 1 & 0 \\ 0 & a_i/a_j \end{bmatrix}\begin{bmatrix} \psi \\ a_j\psi' \end{bmatrix}\equiv\underline{T}_{ij}\begin{bmatrix} \psi \\ a_j\psi' \end{bmatrix} . \tag{11}$$

This defines the boundary transfer matrices $\underline{T}_{12}$ and $\underline{T}_{21}$. In the special case of equal lattice constants they reduce to the unit matrix, of course.

In terms of the transfer matrices now defined, the transfer matrix $\underline{T}_s$ for the complete superlattice unit cell (starting at the origin) takes the form

$$\underline{T}_s=\underline{T}_{12}\underline{T}_2^{p_2}\underline{T}_{21}\underline{T}_1^{p_1} . \tag{12}$$

Allowed bands in the superlattice correspond to complex eigenvalues of $\underline{T}_s$, which requires

$$|\mathrm{tr}\underline{T}_s|\le 2 . \tag{13}$$

We must, therefore, evaluate the trace of (12).

To prepare for this, we introduce a convenient parametrization of the transfer matrices (9). Since

$$\mathrm{tr}\underline{T}_i=2(\underline{T}_i)^{11}=2(\cos q_i-\alpha_i q_i^{-1}\sin q_i) , \tag{14}$$

the expression in parentheses is less than or equal to unity in absolute value in a band of bulk material i. For an energy that corresponds to a band in pure material i we introduce a positive auxiliary variable u_i via

$$\cos u_i=|\cos q_i-\alpha_i q_i^{-1}\sin q_i|,\quad 0\le u_i<\pi/2 , \tag{15}$$

and also for notational purposes the off-diagonal element

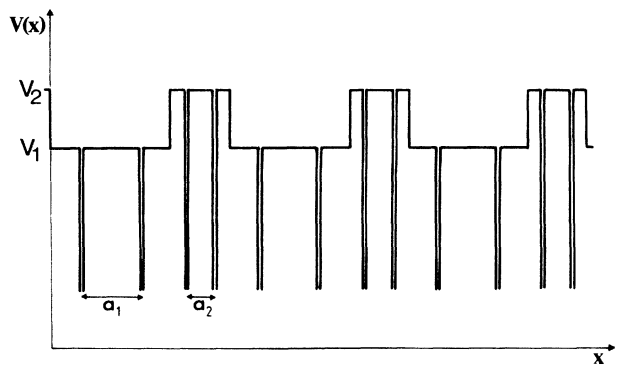

FIG. 2. The periodic potential.

$$b_i\equiv(\underline{T}_i)^{12}=q_i^{-1}\sin q_i-\alpha_i q_i^{-2}+\alpha_i q_i^{-2}\cos q_i . \tag{16}$$

Since each transfer matrix $\underline{T}_i$ has determinant 1, we may write (material-type label i now omitted)

$$\underline{T}=\begin{bmatrix} \eta\cos u & b \\ -b^{-1}\sin^2 u & \eta\cos u \end{bmatrix} , \tag{17}$$

where

$$\eta=\mathrm{sgn}(\underline{T}^{11})=\pm 1 . \tag{18}$$

The two eigenvalues of $\underline{T}$ are readily found to be

$$\lambda_\pm=\eta e^{\pm iu} . \tag{19}$$

The variable u will be useful later on, in the comparison between the exact microscopic results and the effective-mass result. We note that band edges in a homogeneous bulk material correspond to $u=0$. And the sign variable η distinguishes whether the band edge corresponds to the center or the boundary of the Brillouin zone. From the dispersion-relation connection between the Bloch wave vector k and the energy,

$$\cos(ka)=\tfrac{1}{2}\mathrm{tr}\underline{T}=\eta\cos u , \tag{20}$$

we see that $\eta=1$ corresponds to a band edge at $k=k^c=0$ and $\eta=-1$ corresponds to a band edge at $k=k^c=\pm\pi/a$ in the bulk materials. In both cases,

$$\cos u=\cos[(k-k^c)a] . \tag{21}$$

For multiplicative purposes we need to diagonalize the transfer matrix (17). It is easy to show that

$$\underline{T}=\underline{S}\begin{bmatrix} \lambda_+ & 0 \\ 0 & \lambda_- \end{bmatrix}\underline{S}^{-1}$$

with

$$\underline{S}=\begin{bmatrix} b & b \\ i\eta\sin u & -i\eta\sin u \end{bmatrix} . \tag{22}$$

A similar parametrization will be useful for energies that correspond to a *gap* in pure bulk material i. In this case the trace of $\underline{T}_i$ exceeds 2 in magnitude and instead of (15) we introduce an auxiliary variable v_i via

$$\cosh v_i=|\cos q_i-\alpha_i q_i^{-1}\sin q_i|,\quad v_i\ge 0 . \tag{23}$$

The eigenvalues are now real:

$$\lambda_\pm=\eta e^{\pm v} ,$$

again omitting the material-type labels i, and the previous

relations (17)–(22) hold under the replacement $u \rightarrow -iv$. For notational simplicity we use the u variables throughout, and make this replacement when necessary.

It is now a straightforward matter to evaluate the trace of the superlattice transfer matrix (12). The most interesting energy regions are those which correspond to a band in one material and to a gap in the other material. In these energy regions superlattice minibands are expected to occur. If, to be definite, we assume that the energy corresponds to a band in homogeneous material 1 and to a gap in homogeneous material 2, then the variable u_2 will be imaginary below. Inserting the now diagonalized matrices into (12), it is a matter of straightforward algebra to verify the result:

$$|\mathrm{tr}\underline{T}_s| = \left| 2\cos(p_1u_1)\cos(p_2u_2) - \eta_1\eta_2\sin(p_1u_1)\sin(p_2u_2)\left[\frac{a_2b_2\sin u_1}{a_1b_1\sin u_2} + \frac{a_1b_1\sin u_2}{a_2b_2\sin u_1}\right]\right| . \tag{24}$$

The band structure for the superlattice now follows from this exact expression. Bands exist for those energies where the trace (24) does not exceed 2 in absolute value.

We return to this relation for comparison after we have carried through the effective-mass treatment of the same model.

B. Solution of the effective-mass equation

For the superlattice problem the effective-mass stationary Schrödinger equation (5) takes the form

$$-\tfrac{1}{2}\hbar^2 m^{\alpha}\frac{d}{dx}m^{\beta}\frac{d}{dx}m^{\alpha}\phi = [E - E^c(x)]\phi . \tag{25}$$

Here, $E^c(x)$ denotes the local conduction-band edge for the material at position x (we have electrons in mind; for holes the valence-band edge would be relevant). For the present model both $E^c(x)$ and the effective mass $m(x)$ are piecewise-continuous functions. The band edge takes the values E_1^c and E_2^c (Fig. 3), while the effective mass is m_1 and m_2, respectively, in the two materials. Both band edges and effective masses can be expressed in terms of the microscopic parameters of the model (see below).

The boundary conditions associated with the Schrödinger equation (25) are

$$m^{\alpha}\phi = \text{continuous}; \quad m^{\beta}\frac{d}{dx}m^{\alpha}\phi = \text{continuous} . \tag{26}$$

Unless these conditions are met, the left-hand side of (25) will contain stronger singularities than the right-hand side.

The transfer-matrix technique is once more the appropriate tool. Across a single layer of material i the potential is constant. Hence the state vector

$$\begin{bmatrix} \phi \\ a_i\phi' \end{bmatrix} \tag{27}$$

transfers across the layer with the previous transfer matrix (9), with $\alpha_i = 0$. Since the width of the layer is $p_i a_i$ rather than a_i, the transfer matrix now takes the form

$$\underline{t}_i = \begin{bmatrix} \cos(p_i\bar{q}_i) & \bar{q}_i^{-1}\sin(p_i\bar{q}_i) \\ -\bar{q}_i\sin(p_i\bar{q}_i) & \cos(p_i\bar{q}_i) \end{bmatrix} . \tag{28}$$

Here the dimensionless $\bar{q}_i$ (real or imaginary) is defined by

$$\frac{\hbar^2}{2m_i a_i^2}\bar{q}_i^{\,2} = E - E_i^c . \tag{29}$$

We note that the eigenvalues are simply

$$\lambda_{\pm} = e^{\pm ip_i\bar{q}_i} \tag{30}$$

in this case. The transfer matrix (28) can be written in the suggestive form

$$\underline{t}_i = \underline{s}\begin{bmatrix} e^{i\bar{q}_i} & 0 \\ 0 & e^{-i\bar{q}_i} \end{bmatrix}^{p_i}\underline{s}^{-1} , \tag{31}$$

with

$$\underline{s} = \begin{bmatrix} 1 & 1 \\ i\bar{q}_i & -i\bar{q}_i \end{bmatrix} . \tag{32}$$

The form is suggestive because (31) expresses the effective-mass transfer matrix in material i (of width p_i unit cells) as the p_ith iterate of another matrix. We return to this in Sec. II C.

In addition, the boundary conditions (26) must be taken into account. They are conveniently expressed as a transformation of the state vector (27) across each interface. The boundary conditions require that a state vector in material i must be multiplied by an interface matrix

$$\underline{t}_{ji} = \left(\frac{m_i}{m_j}\right)^{\alpha}\begin{bmatrix} 1 & 0 \\ 0 & (m_i/m_j)^{\beta}a_j/a_i \end{bmatrix} \tag{33}$$

when crossing into material j.

The transfer matrix for the complete unit cell of the superlattice now takes the form

$$\underline{t}_s = \underline{t}_{12}\underline{t}_2\underline{t}_{21}\underline{t}_1 , \tag{34}$$

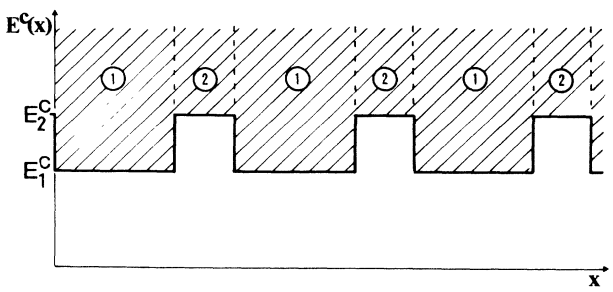

FIG. 3. The conduction-band profile $E^c(x)$.

and it is, once more, necessary to evaluate the trace of this unit-cell transfer matrix. Direct matrix multiplication yields the trace

$$\mathrm{tr}\underline{t}_s = 2\cos(p_1\bar{q}_1)\cos(p_2\bar{q}_2) - \sin(p_1\bar{q}_1)\sin(p_2\bar{q}_2)\left[\frac{a_2}{a_1}\frac{m_1^\beta}{m_1^\beta}\frac{\bar{q}_1}{\bar{q}_2}+\frac{a_1}{a_2}\frac{m_2^\beta}{m_1^\beta}\frac{\bar{q}_2}{\bar{q}_1}\right] . \tag{35}$$

The main question is now to what extent the effective-mass condition for allowed energies,

$$|\mathrm{tr}\underline{t}_s| \le 2 , \tag{36}$$

based on the expression (35), is equivalent to the exact microscopic condition (13).

C. Comparison

In order to compare the exact microscopic expression (24) with the corresponding effective-mass result (35), we must determine the quantities that enter the latter, viz., the conduction-band edges E_i^c and the effective masses m_i of the bulk materials.

The effective mass m at a band minimum at $k=k^c$ is defined by the expansion of the dispersion relation

$$E(k)=E^c+\frac{\hbar^2}{2m}(k-k^c)^2+\cdots . \tag{37}$$

The properties of a homogeneous Kronig-Penney model are well known. Band minima occur for

$$q_{i,n}^c = n\pi, \quad n=1,2,3,\ldots . \tag{38}$$

It is easily seen that the trace of the transfer matrix (9) equals $2(-1)^n$ in these cases. The corresponding energies are

$$E_{i,n}^c = V_i+\frac{\hbar^2}{2m_0a_i^2}n^2\pi^2 . \tag{39}$$

In addition, there is a lowest band ($n=0$) with a band minimum $E_{i,0}^c < V_i$, which cannot be expressed so explicitly.

By expanding the dispersion relation

$$\cos(ka)=\cos q-\alpha q^{-1}\sin q \tag{40}$$

around the band minimum at $k=k^c$ and around $q^c=n\pi$, one finds the effective masses

$$m=m_0\frac{\alpha}{n^2\pi^2}, \quad n=1,2,3,\ldots . \tag{41}$$

at these conduction-band edges. Again the effective mass for the $n=0$ band is less explicit.

Since our strategy is to test the effective-mass procedure in the simplest possible situation, we restrict ourselves to the case $n>0$, and to energies in the neighborhood of the *same* conduction-band edge in both materials (i.e., the same n).

Both the exact treatment and the effective-mass procedure contains a matrix that is iterated p_i times. The eigenvalues of this matrix are $\pm e^{\pm iu_i}$ and $e^{\pm i\bar{q}_i}$, respectively [Eqs. (19) and (30)]. It is natural to suppose that agreement can only be obtained if $u_i=|\bar{q}_i|$. It is not difficult, however, to see that this is not fulfilled. In the effective-mass treatment $\bar{q}_i$ is related to the energy via

$$E=E_{i,n}^c+\frac{\hbar^2\bar{q}_i^2}{2m_ia_i^2} , \tag{42}$$

while in the exact treatment u_i is defined by

$$\cos u_i=|\cos q_i-\alpha q_i^{-1}\sin q_i| , \tag{43}$$

where the energy is related to q_i via

$$E=V_i+\frac{\hbar^2}{2m_0a_i^2}q_i^2=E_{i,n}^c+\frac{\hbar^2}{2m_0a_i^2}(q_i^2-n^2\pi^2) . \tag{44}$$

It is obvious that for a general energy, E, u_i will be different from $\bar{q}_i$. However, *near a band edge*, u_i will be asymptotically equal to $\bar{q}_i$. This is easily shown by expansion of (43) and (44) in $(q_i-n\pi)$ to first order, and elimination of q_i. More elegantly, one can use that since $u_i=a_i|k-k^c|$, Eq. (21), the expansion (37) of the energy in $(k-k^c)$ is equivalent to the expansion

$$E=E_i^c+\frac{\hbar^2}{2m_ia_i^2}u_i^2+\cdots . \tag{45}$$

By comparison between (42) and (45) one concludes that $(u_i/\bar{q}_i)^2\to 1$ when the band edge is approached.

The fact that the effective-mass treatment can only be asymptotically correct for energies in the neighborhood of a band edge (if at all) comes as no surprise, since for *homogeneous* materials this is so. We will consequently restrict our further consideration to this limiting case.

Near the band edge the off-diagonal matrix element b_i, Eq. (16), equals, to lowest nonvanishing order in u_i,

$$b_i=\begin{cases} -2\dfrac{m_i}{m_0} , & n \text{ odd} \quad (46)\\ \dfrac{m_0}{2\pi^2n^2m_i}u_i^2 , & n \text{ even} . \quad (47)\end{cases}$$

Inserting all this into Eq. (24), we have the following condition for band energies for n odd,

$$\left|2\cos(p_1u_1)\cos(p_2u_2)-\sin(p_1u_1)\sin(p_2u_2)\left[\frac{a_2}{a_1}\frac{m_2}{m_1}\frac{u_1}{u_2}+\frac{a_1}{a_2}\frac{m_1}{m_2}\frac{u_2}{u_1}\right]\right| \le 2 , \tag{48}$$

and, for n even,

$$\left|2\cos(p_1u_1)\cos(p_2u_2)-\sin(p_1u_1)\sin(p_2u_2)\left[\frac{a_2}{a_1}\frac{m_1}{m_2}\frac{u_2}{u_1}+\frac{a_1}{a_2}\frac{m_2}{m_1}\frac{u_1}{u_2}\right]\right|\leq 2\ . \tag{49}$$

This is to be compared with the effective-mass condition

$$\left|2\cos(p_1\bar{q}_1)\cos(p_2\bar{q}_2)-\sin(p_1\bar{q}_1)\sin(p_2\bar{q}_2)\left[\frac{a_2}{a_1}\frac{m_1^{\beta}}{m_2^{\beta}}\frac{\bar{q}_1}{\bar{q}_2}+\frac{a_1}{a_2}\frac{m_2^{\beta}}{m_1^{\beta}}\frac{\bar{q}_2}{\bar{q}_1}\right]\right|\leq 2\ . \tag{50}$$

We recall that the variables $\bar{q}_i$ and u_i were shown to be, asymptotically, the same function of the energy E.

For *equal lattice constants* ($a_1=a_2$) the microscopic expressions (48) and (49) coincide, and are identical to the effective-mass condition (50) if, and only if,

$$\beta=-1\ . \tag{51}$$

This answers the question about the form of the effective-mass Hamiltonian in the present case. We must emphasize that the derivation presupposes that the energies in question were close to the band edges (of the pure materials). This can only be fulfilled if the offset

$$V_{\text{off}}=E_2^c-E_1^c \tag{52}$$

is small.

We illustrate this in Fig. 4 by showing the lowest minibands of a superlattice as a function of the offset, evaluated exactly and in the effective-mass approximation.

When the lattice constants are not equal ($a_1\neq a_2$), the microscopic expression (48) for odd-n bands still coincides with the effective-mass condition (50) if $\beta=-1$, but the even-n expression (49) does not agree with condition (50) for any fixed value of β.

We illustrate the difference between odd-n and even-in bands in Fig. 5 by comparing the lower miniband edge, calculated exactly and in the effective-mass approximation, as function of the offset. We see that for $n=1$ the effective-mass treatment (with $\beta=-1$) becomes very accurate for small offsets, but not for $n=2$.

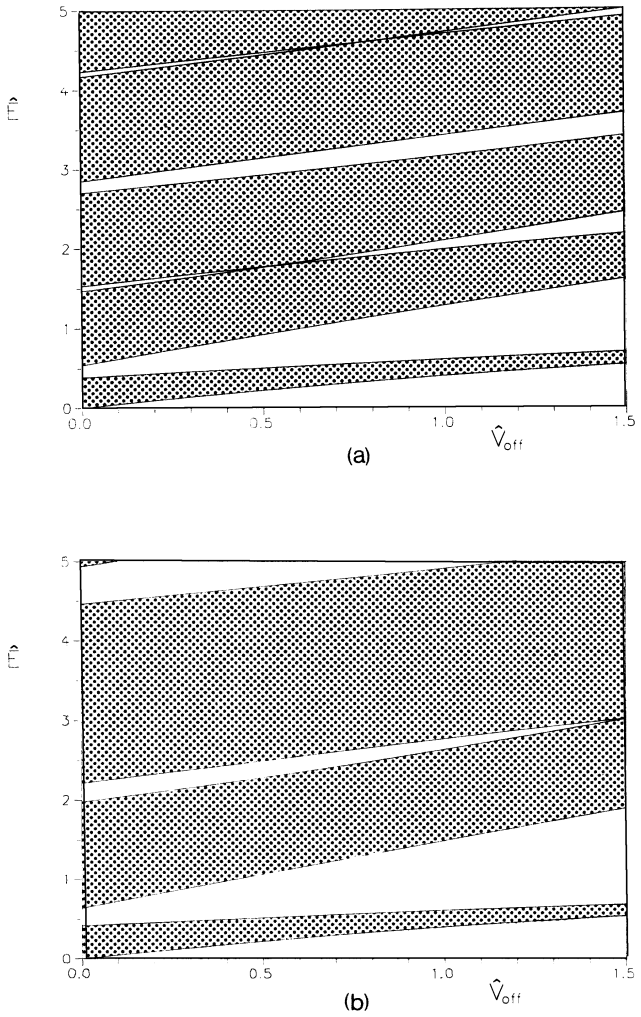

FIG. 4. The miniband structure of a superlattice as function of the offset V_{off} for $a_1=a_2=a$, $\alpha_1=0.5$, $\alpha_2=1$, $p_1=p_2=8$, and $n=1$. Band energies are measured from the band edge in material 1 (well material). Here, $\hat{E}=2m_0a^2E/\hbar^2$ and $\hat{V}_{\text{off}}=2m_0a^2V_{\text{off}}/\hbar^2$ are dimensionless energies. (a) Exact results; (b) effective-mass approximation (with $\beta=-1$).

III. QUANTUM WELLS

A quantum well consists of a well material, material 1, say, with a lower conduction-band edge than the sur-

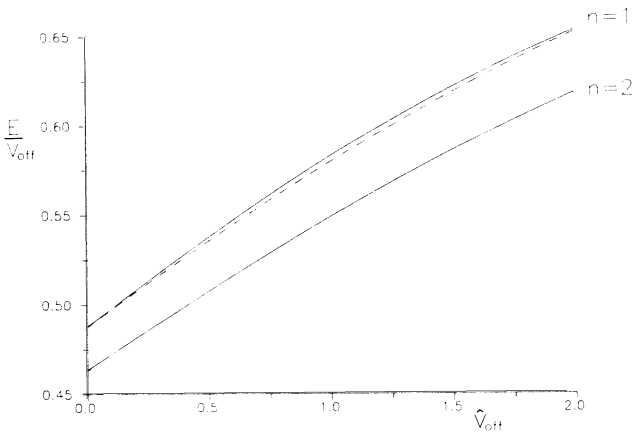

FIG. 5. The lowest miniband edge computed exactly (solid), for an odd-n ($n=1$) and an even-n ($n=2$) band and using the effective-mass approximation (dashed) with $\beta=-1$. Here, $a_2/a_1=1.05$ and $p_1=p_2=8$. For simplicity we have chosen $\alpha_1=0.5,\alpha_2=1$ for $n=1$ and $\alpha_1=2,\alpha_2=4$ for $n=2$ in order to have the same effective masses, and hence the same result from effective-mass theory, in both bands. (The resulting effective masses are $m_1\simeq 0.05m_0$ and $m_2\simeq 0.1m_0$.) Band energies are measured from the band edge of material 2 (barrier material). Here, $\hat{V}_{\text{off}}=2m_0a_2^2V_{\text{off}}/\hbar^2$ is a dimensionless offset. Only for $n=1$ do the two results agree in the limit of zero offset.

rounding material (Fig. 6). The well can support bound states with discrete energy eigenvalues (for the transverse motion). Determination of these energy values can also be used to test the validity and form of the effective-mass equation.

However, this does not really constitute an independent test, since the quantum well can be considered as a limiting case of a superlattice when the width of the barrier increases. Let us consider the $p_2 \to \infty$ limit of the effective-mass inequality (50). First we specialize to energies in the interval of interest, i.e., $E_1^c \le E \le E_2^c$, which implies that $\bar{q}_2$ is purely imaginary. We let $\bar{q}_2 = i\tilde{q}_2$ ($\tilde{q}_2 > 0$), and divide both sides by $\cosh(p_2\tilde{q}_2)$. The result is

$$\left| 2\cos(p_1\bar{q}_1) - \sin(p_1\bar{q}_1)\tanh(p_2\tilde{q}_2) \times \left[\frac{a_2}{a_1}\frac{m_1^\beta}{m_2^\beta}\frac{\bar{q}_1}{\tilde{q}_2} - \frac{a_1}{a_2}\frac{m_2^\beta}{m_1^\beta}\frac{\tilde{q}_2}{\bar{q}_1} \right] \right| \le \frac{2}{\cosh(p_2\tilde{q}_2)} . \tag{53}$$

The limit $p_2 \to \infty$ is now straightforward and turns the inequality into an equality:

$$2\cot(p_1\bar{q}_1) = \frac{a_2}{a_1}\frac{m_1^\beta}{m_2^\beta}\frac{\bar{q}_1}{\tilde{q}_2} - \frac{a_1}{a_2}\frac{m_2^\beta}{m_1^\beta}\frac{\tilde{q}_2}{\bar{q}_1} . \tag{54}$$

We recall that $\bar{q}_1$ and $\tilde{q}_2$ are related to the energy through

$$E = E_1^c + \frac{\hbar^2\bar{q}_1^{\,2}}{2m_1a_1^2} = E_2^c - \frac{\hbar^2\tilde{q}_2^{\,2}}{2m_2a_2^2} . \tag{55}$$

The presence of the lattice constants a_1, a_2 is only apparent. By using $\bar{q}_1/a_1$ and $\tilde{q}_2/a_2$ as variables, one sees that only the total well width a_1p_1 enters the equations.

In precisely the same way the $p_2 \to \infty$ limit of the exact condition (13) can be taken. From Eq. (24) we obtain (for $\eta_1 = \eta_2$)

$$2\cot(p_1u_1) = \frac{a_2}{a_1}\frac{b_2}{b_1}\frac{\sin u_1}{\sinh v_2} - \frac{a_1}{a_2}\frac{b_1}{b_2}\frac{\sinh v_2}{\sin u_1} . \tag{56}$$

It is clear that the effective-mass version (54) and the exact condition (56) can only coincide under precisely the same conditions that we found in the superlattice case, viz., for $\beta = -1$ and for energies close to both band edges.

For equal lattice constants this asymptotic equivalence always holds; for unequal lattice constants it holds only in odd-indexed bands (of the bulk materials).

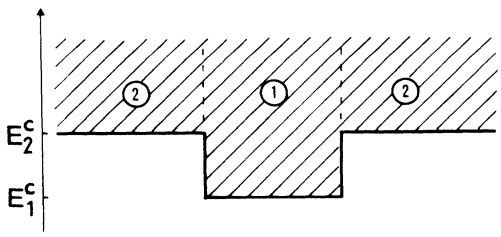

FIG. 6. A quantum well.

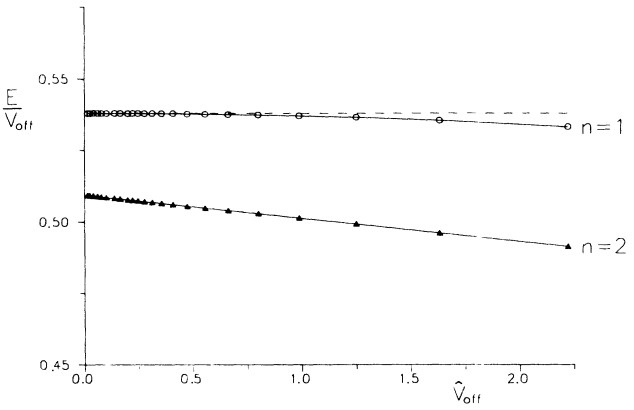

FIG. 7. The quantum-well ground-state energy computed exactly (solid) for an odd-n ($n=1$) band and an even-n ($n=2$) band, and approximately using effective-mass theory (dashed) with $\beta=-1$. Here, $a_2/a_1=1.05$ and $V_{off}=80\hbar^2/2m_0p_1^2a_2^2$. For simplicity we have chosen $\alpha_1=0.5, \alpha_2=1$ for $n=1$ and $\alpha_1=2, \alpha_2=4$ for $n=2$ to have the same effective masses in both cases. Here, $\hat{V}_{off}=2m_0a_2^2V_{off}/\hbar^2$ is a dimensionless offset. The ground-state energies are measured from the band edge of material 2 (barrier). Only for $n=1$ do the effective-mass results agree with the exact results in the zero-offset limit. Data points corresponding to $p_1=6,7,8,\ldots$ are shown.

As an explicit illustration we show in Fig. 7 how the exact and the effective-mass ground-state energy (relative to the barrier band edge) varies with the offset V_{off}.

When n is even, the effective-mass approximation is asymptotically correct only when both materials have the same lattice constant. We make this explicit in Fig. 8 by showing the ratio of the effective-mass result to the exact result (for the ground-state energy) as a function of the lattice constant ratio a_2/a_1 for both an odd-n and an even-n band.

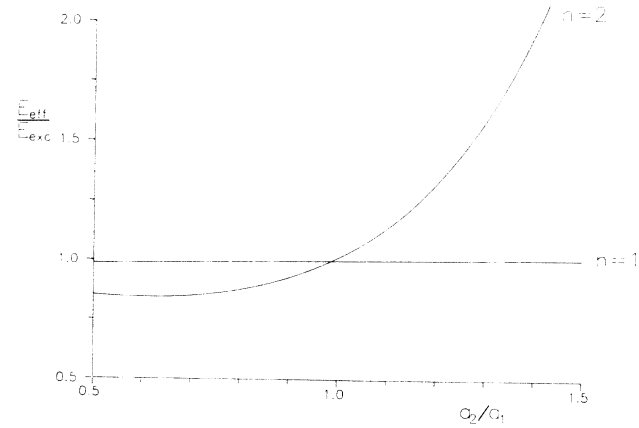

FIG. 8. The ratio of the effective-mass ground-state energy to the exact value for a quantum well, as function of the lattice constant ratio. Here, $\beta=-1$, $p_1=10$, and $V_{off}=(80/p_1^2)(\hbar^2/2m_0a_2^2)$. In order to have the same effective masses for both bands we have used $\alpha_1=0.5$, $\alpha_2=1$ for $n=1$ and $\alpha_1=2, \alpha_2=4$ for $n=2$. Energies are measured from the band edge of material 2 (barrier). The $n=1$ results agree well for all lattice constant ratios. For $n=2$, however, the results agree only for $a_2 \simeq a_1$.

IV. LOCAL POTENTIAL

A. Exact solution

As a final example we consider an electron bound in a potential well $v(x)$ localized near a heterointerface (Fig. 9).

For simplicity we consider a square well,

$$v(x)=\begin{cases}-V_0 & \text{for } -s_2a_2\le x\le s_1a_1\\ 0 & \text{otherwise}\end{cases} \tag{57}$$

with integer width parameters s_1 and s_2. The materials are the same Kronig-Penney materials as in the previous superlattice case.

Let

$$\mathbf{X}_n=\begin{pmatrix}\psi_n\\ a_1\psi_n'\end{pmatrix} \tag{58}$$

be the state vector at position $x=na_1$ in material 1. Starting from X_0 we have

$$\mathbf{X}_{s_1+n}=\underline{T}_1^n(q_1)\underline{T}_1^{s_1}(Q_1)\mathbf{X}_0 . \tag{59}$$

Here, $\underline{T}_1(q)$ is the transfer matrix (9), q_1 is defined in Eq. (10), and we have introduced the new variable

$$Q_i=[2m_0a_i^2(E-V_i+V_0)/\hbar^2]^{1/2} \tag{60}$$

within the range of the square-well potential.

Bound states can only occur for energies E that correspond to a forbidden gap in material 1, where one eigenvalue of the transfer matrix in bulk material 1 is smaller than 1 in magnitude. We diagonalize the $\underline{T}_1$ matrix, Eq. (17), as follows:

$$\begin{aligned}\underline{T}_i(q_1)&=\begin{pmatrix}\eta_1\cosh v_1 & b_1\\ b_1^{-1}\sinh^2 v_1 & \eta_1\cosh v_1\end{pmatrix}\\ &=\tilde{\underline{S}}_1\begin{pmatrix}\eta_1 e^{v_1} & 0\\ 0 & \eta_1 e^{-v_1}\end{pmatrix}\tilde{\underline{S}}_1^{-1},\end{aligned} \tag{61}$$

with

$$\tilde{\underline{S}}_1^{-1}=\begin{pmatrix}\sinh v_1 & b_1\eta_1\\ \sinh v_1 & -b_1\eta_1\end{pmatrix}\frac{1}{2b_1\sinh v_1} . \tag{62}$$

The positive auxiliary variable v_1 is defined in Eq. (23), and $\eta_1=\pm 1$ as before. Inserting the diagonalized form into Eq. (59) we have

$$\mathbf{X}_{s_1+n}=\tilde{\underline{S}}_1\eta_1^n\begin{pmatrix}e^{nv_1} & 0\\ 0 & e^{-nv_1}\end{pmatrix}\tilde{\underline{S}}_1^{-1}\underline{T}_1^{s_1}(Q_1)\mathbf{X}_0 . \tag{63}$$

The wave function decays towards zero when $n\to\infty$ only when the upper component of

$$\tilde{\underline{S}}_1^{-1}\underline{T}_1^{s_1}(Q_1)\mathbf{X}_0 \tag{64}$$

vanishes, which puts a restriction on the initial values ψ_0 and ψ_0':

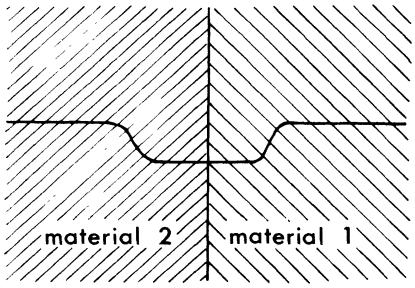

FIG. 9. A localized potential in a heterostructure.

$$\frac{\psi_0'}{\psi_0}=-a_1^{-1}\frac{[\tilde{\underline{S}}_1^{-1}\underline{T}_1^{s_1}(Q_1)]^{11}}{[\tilde{\underline{S}}_1^{-1}\underline{T}_1^{s_1}(Q_1)]^{12}} . \tag{65}$$

Transforming towards $x=-\infty$ instead with the inverse transfer matrices, we obtain a similar condition on ψ_0'/ψ_0 in order for the wave function to decay when $x\to-\infty$. Finally continuity of ψ_0 and ψ_0' at the interface yields the condition for bound states. In the Appendix we show that this condition may be written compactly as

$$\sum_{i=1}^{2}\tilde{\eta}_1\frac{\sin U_i}{a_iB_i}\tan(s_iU_i+\delta_i)=0 . \tag{66}$$

We have defined positive auxiliary variables U_i via

$$\cos U_i=|\cos Q_i-\alpha_iQ_i^{-1}\sin Q_i| , \tag{67}$$

δ_i via

$$\tan\delta_i=-\frac{\tilde{\eta}_iB_i\sinh v_i}{\eta_ib_i\sin U_i} , \tag{68}$$

and B_i the off-diagonal matrix element

$$\begin{aligned}B_i&=[\underline{T}_i(Q_i)]^{12}\\ &=b_i(Q_i)\\ &=Q_i^{-1}\sin Q_i-\alpha_iQ_i^{-2}+\alpha_iQ_i^{-2}\cos Q_i .\end{aligned} \tag{69}$$

Also

$$\tilde{\eta}_i=\operatorname{sgn}[\underline{T}_i(Q_i)]^{11} . \tag{70}$$

We will return to this exact equation for the discrete energy levels after we have determined the corresponding condition in the effective-mass treatment.

B. Solution of the effective-mass equation

Since the potential energy is piecewise constant, the effective-mass Schrödinger equation

$$-\tfrac{1}{2}m^{\alpha}\frac{d}{dx}m^{\beta}\frac{d}{dx}m^{\alpha}\phi=[E-E^c(x)-v(x)]\phi \tag{71}$$

is satisfied by

$$\phi(x)\propto\begin{cases}\exp(\tilde{q}_2x/a_2), & x<-s_2a_2\\ \cos(\tilde{Q}_2x/a_2+c_2), & -s_2a_2<x<0\\ \cos(\tilde{Q}_1x/a_1+c_1), & 0<x<s_1a_1\\ \exp(-\tilde{q}_1x/a_1), & s_1a_1<x .\end{cases} \tag{72}$$

Here,

$$\tilde{q}_i=[2m_i a_i^2(E_i^c-E)/\hbar^2]^{1/2} ,$$
$$\tilde{Q}_i=[2m_i a_i^2(E-E_i^c+V_0)/\hbar^2]^{1/2} , \quad (73)$$

and c_1, c_2 are constants. Connecting the wave function and its derivative at $x=-s_2a_2$, 0, and s_1a_1 in accordance with the boundary conditions (26), we readily obtain the following implicit equation for the bound-state energies E:

$$\sum_{i=1}^{2} m_i^{\beta}\frac{\tilde{Q}_i}{a_i}\tan(\tilde{Q}_i s_i+\tilde{\delta}_i)=0 , \quad (74)$$

with

$$\tan\tilde{\delta}_i=-\tilde{q}_i/\tilde{Q}_i . \quad (75)$$

C. Comparison

The exact and the effective-mass results do not coincide, but once more we want to investigate whether conditions exist so that they are essentially in agreement. As in the superlattice case we expect that only for energies in the neighborhood of a band edge can the effective-mass treatment be asymptotically correct, if at all. Thus both the offset and the potential strength V_0 are assumed small.

This motivates an expansion in the auxiliary variables v_i, which vanish at the appropriate band edges. The exact relation

$$Q_i^2-q_i^2=2m_0a_i^2\hbar^{-2}V_0 \quad (76)$$

shows that Q_i is close to q_i when V_0 is small. It follows that U_i is close to v_i and can consequently also be considered small in this limiting case. We have already obtained in Eqs. (46) and (47) the expansion of the off-diagonal elements b_i, and in complete analogy we obtain to lowest order in U_i

$$B_i=\begin{cases} -2\dfrac{m_i}{m_0}, & n \text{ odd} \\ \dfrac{m_0}{2\pi^2n^2m_i}U_i^2, & n \text{ even} . \end{cases} \quad (77)$$

The positive integer n is the band index, assumed to be the same in each material. Thus the sign variables $\eta_i, \tilde{\eta}_i$ are the same in both materials.

By use of (46) and (77) the exact relation (66) takes, for *odd n*, the asymptotic form

$$\sum_{i=1}^{2}\frac{U_i}{a_i m_i}\tan(s_i U_i+\delta_i)=0 , \quad (78)$$

with

$$\tan\delta_i=-v_i/U_i . \quad (79)$$

We also recall the connection between the energy parameter and the auxiliary variables v_i, U_i. Equivalent to Eq. (45), we have

$$E=E_i^c-\frac{\hbar^2}{2m_i a_i^2}v_i^2+\cdots=E_i^c-V_0+\frac{\hbar^2}{2m_i a_i^2}U_i^2+\cdots . \quad (80)$$

The set of equations (78)–(80) is, except for notation ($U_i\to\tilde{Q}_i$, $v_i\to\tilde{q}_i$, $\delta_i\to\tilde{\delta}_i$), *exactly* the effective-mass conditions (73)–(75), with, most importantly,

$$\beta=-1 . \quad (81)$$

We note, however, from Eq. (80) that only when the offset $E_2^c-E_1^c$ vanishes can one obtain *exact* asymptotic equivalence for $V_0\to 0$. This is illustrated in Fig. 10. The figure shows clearly that in the presence of an offset, the ratio of the effective-mass binding energy to the exact binding energy does not approach unity in the shallow-potential limit, in contrast to the zero-offset case with $\beta=-1$.

This was for an odd-n band. For *even n*, the off-diagonal matrix elements b_i vanish at band edges. By use of expansion (47), and similarly of (77) for B_i, the exact relation takes the asymptotic form

$$\sum_{i=1}^{2}\frac{m_i}{a_i U_i}\tan(s_i U_i+\delta_i)=0 \quad (82)$$

with

$$\tan\delta_i=U_i/v_i . \quad (83)$$

By taking the inverse of (82) a more convenient form is obtained:

$$\sum_{i=1}^{2}\frac{a_i U_i}{m_i}\tan(s_i U_i+\kappa_i)=0 \quad (84)$$

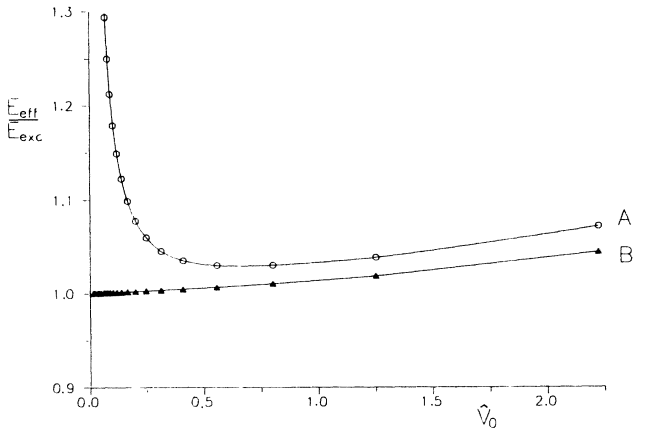

FIG. 10. A comparison of the ground-state energies $E_{\text{eff}}, E_{\text{exc}}$ for a localized potential determined via the effective-mass equation (74) with $\beta=-1$, and by the exact relation (66), respectively. We consider the lowest gap ($n=1$) and have taken $\alpha_1=0.5, \alpha_2=1$. The square potential is symmetrically situated ($s_1=s_2=s, a_1=a_2=a$) with a depth chosen to be $V_0=20\hbar^2/2m_0a^2s^2$. Data points corresponding to $s=3,4,5,\ldots$ are shown. Here $\hat{V}_0=2m_0a^2V_0/\hbar^2$ is a dimensionless potential depth. Ground-state energies are measured from the lower band edge. *A*, with offset ($E_1^c-E_2^c=0.5\hbar^2/2m_0a^2$); *B*, without offset ($E_1^c=E_2^c$).

with

$$\tan\kappa_i = -v_i/U_i \ . \tag{85}$$

This is precisely the same relation as obtained in the odd-n case, with one small difference. The difference is that the lattice constants a_i that occur in the denominator in (78) now appear in the numerator in (84).

In the case of *equal lattice constants* the conclusion is the same as above: With zero offset and with $\beta=-1$ the effective-mass treatment is asymptotically exact.

In the case of *unequal lattice constants,* however, this is no longer true. We illustrate this in Fig. 11 for a lattice-constant ratio of 1.25. The shallow-potential limit $V_0\to 0$ produces asymptotic equivalence in the $n=1$ case, not for $n=2$.

D. Another interface setup

In order to check, at least to some extent, whether the conclusions are dependent upon the details of the model, we have also investigated a different setup. (The results for this case, with equal lattice constants, have already been reported.[17])

In this alternative version the interface is *at* a δ-function well instead of between two wells:

$$V(x)=\begin{cases} V_1-\dfrac{\hbar^2\alpha_1}{m_0 a_1}\displaystyle\sum_{n=1}^{\infty}\delta(x-na_1), & x>0 \\ -\dfrac{\hbar^2}{2m_0}\left[\dfrac{\alpha_1}{a_1}+\dfrac{\alpha_2}{a_2}\right]\delta(x), & \\ V_2-\dfrac{\hbar^2\alpha_2}{m_0 a_2}\displaystyle\sum_{n=-\infty}^{-1}\delta(x-na_2), & x<0 \ . \end{cases} \tag{86}$$

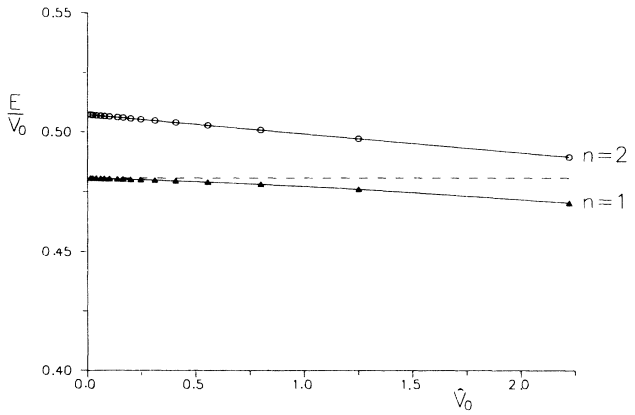

FIG. 11. The ground-state energy of a localized potential computed via the exact relation (66) (solid) and via the effective-mass equation (74) (dashed) with $\beta=-1$, respectively. Here $a_2/a_1=1.25$ and $s_1=s_2=s$, and the depth is chosen to be $V_0=20\hbar^2/2m_0a_2^2s^2$. We have chosen $\alpha_1=0.5,\alpha_1=1$ for $n=1$ and $\alpha_1=2,\alpha_2=4$ for $n=2$ in order to have the same effective masses for both bands. The offset is adjusted to zero. Data points correspondoing to $s=3,4,5,\ldots$ are shown. Here, $\hat{V}_0=2m_0a_2^2V_0/\hbar^2$ is a dimensionless potential depth. Ground-state energies are measured from the band edges. One obtains asymptotic agreement in the zero-offset limit only for $n=1$.

The strength of the interface δ-function well has been chosen as the average of the potential strengths in the two materials.

The effective-mass treatment is of course the same as before, but the exact calculation gives a different result. In this case it is natural to use a transfer matrix that transfers the state vector from one δ well to the neighboring δ well (since the derivative is discontinuous at the δ well we use the derivative on the right-hand side of each well). The transfer matrix

$$\underline{T}_i(q_i)=\begin{pmatrix} \cos q_i & q_i^{-1}\sin q_i \\ -q_i\sin q_i-2\alpha_i\cos q_i & \cos q_i-2\alpha_i q_i^{-1}\sin q_i \end{pmatrix} \tag{87}$$

does the job. The trace of the previous transfer matrix (9) and the new one (87) is the same, of course.

The procedure for determining bound state is essentially the same as before. One starts with a state vector X_0^+ at the interface (at $x=0+$), and selects the initial condition that secures a decreasing wave function when transforming $x=+\infty$. Transforming towards $x=-\infty$, one finds a similar condition on the state vector X_0^- at $x=0^-$. Finally the difference $(\psi'_{0+}-\psi'_{0-})/\psi_0$ is given by the strength of the δ function at the interface.

After some algebra this yields the following exact condition for bound states:

$$\sum_{i=1}^{2}\frac{Q_i}{a_i}\frac{\sin U_i}{\sin Q_i}\tan(s_iU_i+\tilde{\kappa}_i)=0 \ , \tag{88}$$

where

$$\tan\tilde{\kappa}_i=-\frac{q_i}{\sin q_i}\frac{\sin Q_i}{Q_i}\frac{\sinh v_i}{\sin U_i} \ . \tag{89}$$

Condition (88) is analogous to Eq. (66) for the previous setup. Although the two expressions are different, the expansion of (88) in terms of deviations from the (essentially coinciding) band edges yields, to lowest order, precisely the result (82), obtained previously for *even* n.

The conclusion, therefore is now for all band indices n, the same as for the previous even-n case: For *equal* lattice constants the effective-mass treatment is asymptotically exact (in the vanishing offset limit). With unequal lattice constants this asymptotic agreement does not hold. Figure 12 corresponds to Fig. 10 for the previous setup, and one sees that the qualitative aspects are identical and the quantitative results similar.

V. SUMMARY AND DISCUSSION

In the present article we have compared exact model calculations with results based upon the effective-mass Hamiltonian (5).

One main result is that the effective-mass equation yields, under certain conditions, asymptotically exact results, provided the parameters take the values $\alpha=0$, $\beta=-1$. Assuming the parameter values to be universal, this selects uniquely the following form for the kinetic operator:

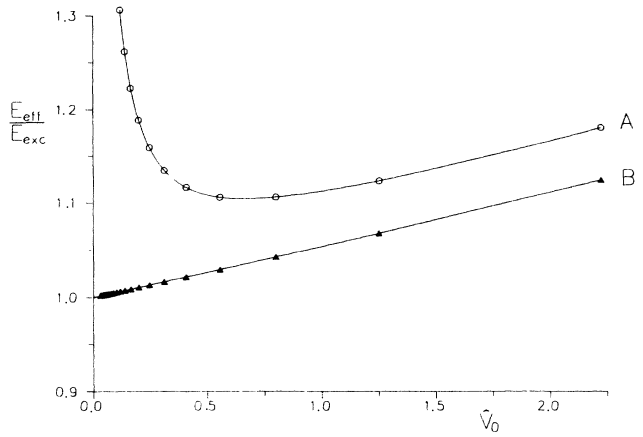

FIG. 12. A comparison of ground-state energies $E_{\text{eff}}, E_{\text{exc}}$ for a localized potential determined via the effective-mass equation (74) with $\beta=-1$, and by the exact relation (88) for the new interface setup, respectively. We consider the lowest gap ($n=1$) and have taken $\alpha_1=0.5, \alpha_2=1$. The square potential is symmetrically situated ($s_1=s_2=s, a_1=a_2=a$) with a depth chosen to be $V_0=20\hbar^2/2m_0a^2s^2$. Data points corresponding to $s=3,4,5$ are shown. Here, $\hat{V}_0=2m_0a^2V_0/\hbar^2$ is a dimensionless potential depth. Ground-state energies are measured from the lower band edge. *A*, with offset ($E_1^c-E_2^c=0.5\hbar^2/2m_0a^2$); *B*, without offset ($E_1^c=E_2^c$).

$$H_{\text{kin}}=-\frac{\hbar^2}{2}\nabla\frac{1}{m(\mathbf{r})}\nabla \ . \tag{90}$$

This form was apparently first used by BenDaniel and Duke.[18]

While most efforts on deciding the form of the kinetic operator have been purely theoretical, some approaches have also involved the utilization of experimental data. Galbraith and Duggan[8] compared effective-mass results parametrized by β with photoluminescence excitation spectra from GaAs-$Al_{0.35}Ga_{0.65}As$ quantum wells and found $\beta\approx-1$ to give the best fit. In the same spirit, Fu and Chao[9] tried to determined β using optical data for a set of GaAs-$Al_xGa_{1-x}As$ superlattices but found for these cases the effective-mass results to be too insensitive to the value of β to give a conclusive answer.

One condition for the effective-mass theory to work is that the energies in question are close to both band edges. A second condition is equality of the lattice constants. Although the second condition is often well fulfilled in practical circumstances it remains to construct an effective-mass type theory for strained heterostructures. As is shown in an accompanying article,[19] the present results suggest how a modified effective-mass treatment, with asymptotic validity, may be constructed.

APPENDIX

In evaluating expression (65), we must raise the transfer matrix to an arbitrary power s:

$$\underline{T}^s(Q)=\begin{bmatrix}\tilde{\eta}\cos U & B\\ -B^{-1}\sin^2U & \tilde{\eta}\cos U\end{bmatrix}^s$$
$$=\tilde{\eta}^s\begin{bmatrix}\cos(sU) & \tilde{\eta}B\sin(sU)/\sin U\\ -\tilde{\eta}B^{-1}\sin(sU)\sin U & \cos(sU)\end{bmatrix} .$$

This is shown in a straightforward manner by first diagonalizing $\underline{T}(Q)$, as in Eq. (22). We have used the abbreviation (69) for the upper nondiagonal element, and have omitted the material type label.

Multiplication by $\tilde{\underline{S}}^{-1}$, Eq. (62), and insertion into (65) yields

$$a_1\psi_0'/\psi_0=h(1) ,$$

with

$$h(1)=\frac{-\sin U_1\sinh v_1+b_1\eta_1\tilde{\eta}_1B_1^{-1}\sin^2U_1\tan(s_1U_1)}{\sinh(v_1)\tilde{\eta}_1B_1\tan(s_1U_1)+b_1\eta_1\sin U_1} .$$

This may be written

$$h(1)=\frac{\tilde{\eta}_1\sin U_1}{B_1}\tan(s_1U_1+\delta_1) ,$$

where

$$\tan\delta_1=-\frac{\tilde{\eta}_1B_1\sinh v_1}{\eta_1b_1\sin U_1} .$$

Transforming towards $x=-\infty$ instead, we must obtain by symmetry the equivalent result in material 2, except for an overall sign. Continuity of ψ_0 and ψ_0' at the interface leads to

$$\frac{h(1)}{a_1}+\frac{h(2)}{a_2}=0 ,$$

which is the condition (66) for the discrete energy eigenvalues.

[1]G. H. Wannier, Phys. Rev. **52**, 191 (1937); H. M. James, *ibid.* **76**, 1611 (1949); J. C. Slater, *ibid.* **76**, 1592 (1949); J. M. Luttinger and W. Kohn, *ibid.* **97**, 869 (1955).

[2]See, G. Bastard, *Wave Mechanics Applied to Semiconductor Heterostructure* (Les Editions de Physique, Les Ulis, France, 1988) and references therein.

[3]R. A. Morrow and K. R. Brownstein, Phys. Rev. B **30**, 678 (1984).

[4]R. A. Morrow, Phys. Rev. B **35**, 8074 (1987).

[5]R. A. Morrow, Phys. Rev. B **36**, 4836 (1987); P. Enders, Phys. Status Solidi B **139**, K113 (1987); H. C. Liu, Superlatt. Microstruct. **3**, 413 (1987).

[6]M. G. Burt, Semicond. Sci. Technol. **3**, 739 (1988).

[7]W. Trzeciakowski, Phys. Rev. B **38**, 4322 (1988).

[8]I. Galbraith and G. Duggan, Phys. Rev. B **38**, 10057 (1988).

[9]Y. Fu and K. A. Chao, Phys. Rev. B **40**, 8349 (1989).

[10]K. Young, Phys. Rev. B **39**, 13 434 (1989).
[11]J. Thomsen, G. T. Einevoll, and P. C. Hemmer, Phys. Rev. B **39**, 12 783 (1989).
[12]O. von Roos, Phys. Rev. B **27**, 7547 (1983).
[13]S. R. White and L. J. Sham, Phys. Rev. Lett. **47**, 879 (1981).
[14]K. B. Kahen and J. P. Leburton, Phys. Rev. B **33**, 5465 (1986).
[15]Q.-G. Zhu, and H. Kroemer, Phys. Rev. B **27**, 3519 (1983).
[16]T. Ando and S. Mori, Surf. Sci. **113**, 124 (1982).
[17]G. T. Einevoll and P. C. Hemmer, J. Phys. C **21**, L1193 (1988).
[18]D. J. BenDaniel and C. B. Duke, Phys. Rev. **152**, 683 (1966).
[19]G. T. Einevoll, this issue, the following paper, Phys. Rev. B **42**, 3497 (1990).